

# Dynamic Soaring in the Atmospheric Boundary Layer – an Experimental Investigation: with an Appendix on Wind Shear

by Vadym V. Utgoff, Associate Professor, Aerospace Engineering Department, U.S. Naval Academy and Frederick G. Johnson, Midshipman, USN, U.S. Naval Academy

Presented at the XV OSTIV Congress, Räyskälä, Finland (1976)

## Abstract

The feasibility of maintaining continuous non-powered flight by utilizing a vertical wind velocity gradient is analyzed. It is concluded that wind velocity gradients which have been observed in the upper atmosphere are not sufficiently steep for this purpose; but wind shears likely to be encountered in the surface boundary layer should be adequate.

A suitable flight pattern was developed and an experimental investigation was conducted utilizing a powered aeroplane with the power adjusted to simulate existing and advanced sailplanes. Zero net loss of altitude was not attained, but it was concluded that further investigation is warranted with particular attention directed towards precise adherence to the prescribed flight pattern.

## Nomenclature

a	exponent of boundary layer shear equation; based upon terrain considerations
AR	aspect ratio
$C_{Dmin}$	drag coefficient at zero lift
$C_L$	lift coefficient
D	drag
E	energy
$E_a$	available wind energy
$E_d$	energy dissipated to drag
e	span efficiency factor
F	force acting on the aircraft due to wind shear
$F_x$	force in the x direction
$F_y$	force in the y direction
f	Phugoid frequency
g	acceleration due to gravity
h	altitude
k	strength coefficient of boundary layer shear power equation
L	lift
P	power
$P_a$	power available
$P_d$	power required
R/S	rate of sink
S	wing surface area
t	time
V	true airspeed
$V_o$	true airspeed for minimum sink
$V_g$	ground speed
$V_w$	wind speed
W	weight

$\delta$	Phugoid phase angle
$\gamma$	flight angle
$\rho$	density
$\psi$	flight heading with respect to wind direction
$\Omega$	angular rotation rate (turning rate)

## Introduction

The possibility of dynamic soaring, utilization of wind shear to maintain flight without power, has been an intriguing concept ever since it was observed that certain sea birds, for example the albatross *Diomedea*, remained airborne with a minimum expenditure of energy by flying within the atmospheric boundary layer and varying altitude in a periodic cycle.

The fundamentals of the required analysis were set forth by Rayleigh in 1883. More refined analyses have appeared in the literature subsequently. There appears to be no theoretical obstacle to achieving this mode of flight in a man-made vehicle.

Experimental investigation of the possibility of dynamic soaring in the atmospheric boundary layer has been inhibited, however, by a very practical consideration. In the atmospheric boundary layer, as in any boundary layer, the steepest wind velocity gradient occurs near the surface. Since flight utilizing wind shear requires a fairly high value of the latter, an experimental investigation of this phenomenon must be conducted close to the surface. For obvious reasons, investigators appear reluctant to attempt this in aircraft without power. The investigation reported in this paper was made close to the surface of the sea in a powered aircraft. The velocity profile of the boundary layer was determined for each flight by making observations of the wind velocity at various altitudes.

A flight pattern was then set up within the region of greatest wind shear. It consisted of a circular pattern of ascending flight upwind and descending flight downwind. Power settings were varied as necessary to simulate glide ratios covering the range of contemporary sailplanes and possible future developments.

## Analysis

The problem of utilizing a vertical wind velocity gradient to provide the energy required to maintain unpowered flight can best be put into perspective by considering a very simple case: steady climb or descent at constant true airspeed and pitch attitude through a positive velocity gradient. The climb is made into the wind. To simplify the problem further this will be assumed to be linear, as shown.

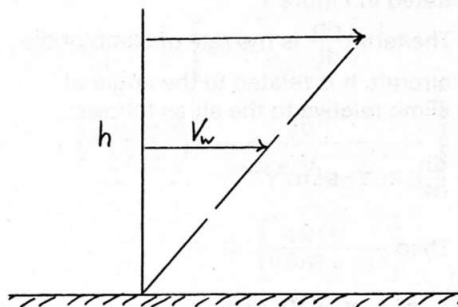


Fig. 1

The forces acting on the flight vehicle in the climb are shown in Figure 2.

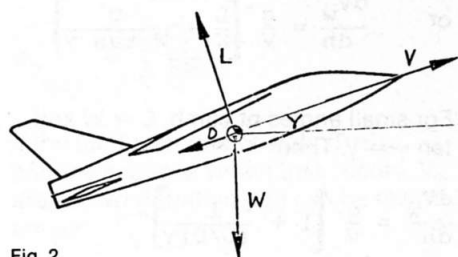


Fig. 2

Summing forces horizontally and vertically

$$\Sigma F_z = L \cos \gamma - D \sin \gamma - W$$

$$\Sigma F_x = -L \sin \gamma - D \cos \gamma$$

If airspeed and pitch attitude are constant, and if there is no vertical wind component, the aircraft is in a steady climb and the vertical acceleration is zero. Hence

$$L \cos \gamma = W + D \sin \gamma$$

In the absence of a propulsive force, the horizontal force summation is obviously not zero. The aircraft will therefore be decelerated, with reference to the ground, in the negative x-direction, as illustrated.

Consider now a balloon rising at a steady rate through the wind shear represented by Figure 1. It will be accelerated in the direction of increasing wind velocity. If the balloon is rising at the rate

$$\frac{dh}{dt}$$

the magnitude of the horizontal acceleration will be

$$\frac{d^2x}{dt^2} = \frac{dV_w}{dh} \frac{dh}{dt}$$

If the aircraft is climbing into the wind, to maintain steady flight its deceleration must be precisely equal to the acceleration of the balloon. Then, from Newton's Second Law

$$L \sin \gamma + D \cos \gamma = \frac{W}{g} \frac{dv_w}{dh} \frac{dh}{dt}$$

The term  $\frac{dv_w}{dh}$  depends on the velocity profile of the wind.

It is constant for the linear profile illustrated in Figure 1.

The term  $\frac{dh}{dt}$  is the rate of climb of the aircraft. It is related to the angle of climb relative to the air as follows:

$$\frac{dh}{dt} = V \sin \gamma$$

Then

$$L \sin \gamma + D \cos \gamma = \frac{W}{g} \left( \frac{dv_w}{dh} V \sin \gamma \right)$$

$$\text{or } \frac{dv_w}{dh} = \frac{g}{V} \left[ \frac{L}{W} + \frac{D}{W \tan \gamma} \right]$$

For small angles of climb,  $L = W$  and  $\tan \gamma = \gamma$ . Then

$$\frac{dv_w}{dh} = \frac{g}{V} \left[ 1 + \frac{1}{(L/D)\gamma} \right]$$

The importance of a high  $L/D$  is readily apparent. The minimum wind velocity gradient required to maintain a steady climb is approached as  $L/D \rightarrow \infty$ . In the limit,

$$\frac{dv_w}{dh} = \frac{g}{V}$$

For any reasonable value of  $V$ , the

required  $\frac{dv_w}{dh}$  thus, derived is two orders

of magnitude larger than anything observed in nature. Thus, a steady climb in a wind shear, without power, appears to be unattainable.

Let us consider another case: A glide downwind through the same condition of wind shear.

Figure 3 shows the balance of forces now.

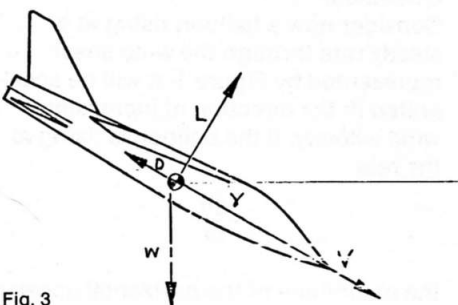


Fig. 3

$$\Sigma F_z = L \cos \gamma + D \sin \gamma - W = 0$$

$$\Sigma F_x = L \sin \gamma - D \cos \gamma$$

The aircraft is again decelerated. As before, the magnitude of this deceleration will be

$$(1) \frac{d^2x}{dt^2} = \frac{dv_w}{dh} \frac{dh}{dt} \quad \text{and}$$

$$\frac{dh}{dt} = \frac{dv_w}{dh} V \sin \gamma$$

The horizontal force summation then becomes

$$-L \sin \gamma + D \cos \gamma = \frac{W}{g} \frac{dv_w}{dh} V \sin \gamma$$

For small angles we may again take  $L = W$  and  $\tan \gamma = \gamma$ .

The resulting expression is the same as the previous one, but may be rearranged to yield

$$(2) \quad \gamma = \frac{1}{L/D \left( 1 + \frac{V}{g} \frac{dv_w}{dh} \right)}$$

It is evident that descending downwind through a positive wind velocity gradient increases the effective  $L/D$ , or reduces the glide angle.

Let us now turn our attention to a flight path copied from the albatross: circling, climbing into the wind, and descending downwind. Figure 4 is a view from above.

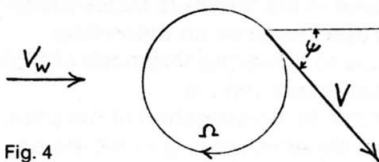


Fig. 4

The ground speed, and acceleration, for any point on the flight path, are given by

$$(3) \quad v_g = V + v_w \cos \psi$$

$$(4) \quad \frac{dv_g}{dt} = \frac{dv}{dt} + \cos \psi \frac{dv_w}{dt} - v_w \sin \psi \frac{d\psi}{dt}$$

In the presence of a wind velocity gradient

$$(5) \quad \frac{dv_w}{dt} = \frac{dv_w}{dh} \frac{dh}{dt}$$

The resulting inertia force due to the wind is

$$(6) \quad F = \frac{W}{g} \left[ \cos \psi \frac{dv_w}{dh} \frac{dh}{dt} - v_w \Omega \sin \psi \right]$$

When  $F < 0$  the aircraft is decelerating in inertial space; thus the wind is supplying energy to it. When  $F > 0$  the aircraft is accelerating, and energy must be supplied to it by loss of altitude or by an engine.

Equation (6) has important consequences in everyday flight operations. The second term in Equation (6) is negative when turning from downwind into the wind, i.e.,  $0 < \psi < 180^\circ$ . This occurs in the landing approach when turning to the base leg and onto final. Even in the absence of wind shear, if there is a steady wind, a net gain in altitude would be experienced, or a power reduction would be necessary. When turning from into the wind to downwind, i.e.,  $180^\circ < \psi < 0^\circ$ , as after take off, this term is positive. Thus, to avoid a decrease in the climb rate, an increase in power is required.

The first term is negative when climbing into the wind or descending with the wind, if the wind velocity increases with altitude, as in the earth's boundary layer. Thus, when descending on the final approach in strong winds, the term is positive, and the descent rate will increase unless additional power is used. This accounts for the well known dangers commonly associated with landing in the presence of wind shear. Turning onto the base leg and onto final approach, the pilot finds his rate of descent is less than expected, so he reduces power to maintain it. Then, when descending on the final approach, the rate of sink is increased above that experienced in still air.

On take-off a similar problem is encountered. The initial climb rate through the wind shear is greater than normal, but this is followed by a sharp decrease when turning out of the wind. It is apparent that power, the deceleration force multiplied by the true air speed, can be extracted from a wind shear by flying in a circular pattern, climbing into the wind and descending downwind. This precisely what the albatross does.

The power thus supplied is

$$(7) \quad P_a = \frac{WV}{g} \left[ \cos \psi \frac{dv_w}{dh} \frac{dh}{dt} - v_w \Omega \sin \psi \right]$$

The flight path described is a pendulum-like oscillation combined with turning flight. Altitude, true airspeed, and pitch attitude vary sinusoidally as follows:

$$(8) \quad h = \bar{h} - \frac{\Delta h}{2} \sin \psi \quad \text{where}$$

$$(9) \quad \Delta h = h_{\max} - h_{\min} \quad \text{and}$$

$$(10) \quad \bar{h} = \frac{h_{\max} + h_{\min}}{2}$$

$$(11) v = \bar{v} + \frac{\Delta V}{2} \sin \psi \quad \text{where}$$

$$(12) \Delta V = v_{\max} - v_{\min} \quad \text{and}$$

$$(13) \bar{v} = \frac{v_{\max} + v_{\min}}{2}$$

$$(14) \gamma = -\gamma_{\max} \cos \psi$$

$v_{\max}$  will generally be the maximum design maneuvering speed of the aircraft.  $v_{\min}$  will be determined by the stalling speed. Altitude, velocity, and pitch variations can be determined as follows:

Excluding the energy lost due to drag, the change in kinetic energy will be equal to the change in potential energy:

$$(15) \Delta h = \frac{v_{\max}^2 - v_{\min}^2}{2g}$$

The relationship between the airspeed at any time and rate of climb or glide may now be determined. The rate of climb or sink at any time is

$$(16) \frac{dh}{dt} = -\left(\frac{dh}{dt}\right)_{\max} \cos \psi$$

$$dh = -\left(\frac{dh}{dt}\right)_{\max} \cos \psi dt$$

But  $\psi = \Omega t$  and  $d\psi = \Omega dt$  so

$$dh = -\frac{1}{\Omega} \left(\frac{dh}{dt}\right)_{\max} \cos \psi d\psi$$

Integrating over  $1/2$  a cycle from  $h_{\max}$  to  $h_{\min}$

$$(17) \Delta h = \frac{2}{\Omega} \left(\frac{dh}{dt}\right)_{\max}$$

Replacing  $\Delta h$  from Equation (15) yields

$$(18) \left(\frac{dh}{dt}\right)_{\max} = \frac{\Omega}{4g} (v_{\max}^2 - v_{\min}^2) \quad \text{and}$$

$$(19) \frac{dh}{dt} = \frac{-\Omega}{4g} (v_{\max}^2 - v_{\min}^2) \cos \psi$$

Equation (7) can now be rewritten as

$$(20) P_a = \frac{W\Omega}{g} \left[ \bar{v} + \frac{\Delta V}{2} \sin \psi \right] \left[ \frac{-1}{4g} \frac{dV}{dh} (v_{\max}^2 - v_{\min}^2) \cos^2 \psi - v_w \sin \psi \right]$$

The total energy supplied by the wind in one complete cycle is

$$(21) E_a = -\int P_a dt = -\frac{1}{\Omega} \int_0^{2\pi} P_a d\psi$$

In order to perform the indicated integration, it is necessary to evaluate

$\frac{dV_w}{dh}$  and  $V_w$  as functions of  $\psi$ .

Wind velocity within the earth's boundary layer can be expressed as

$$v_w = k h^a$$

$$\text{or } v_w = k \left( \bar{h} - \frac{\Delta h}{2} \sin \psi \right)^a$$

where "k" is a strength factor and "a" depends on the nature of the surface over which the wind is blowing. The velocity gradient is

$$\frac{dv_w}{dh} = ak \left( \bar{h} - \frac{\Delta h}{2} \sin \psi \right)^{a-1}$$

For small  $\Delta h$ , however, the wind velocity and the velocity gradient can be taken as constants at their values at the mean altitude. In this case, Equation (21) yields

$$(22) E_a = \pi \frac{W}{g} \left( \frac{\Delta V}{2} \right) \left[ \frac{1}{g} \left( \frac{dv_w}{dh} \right) \bar{v}^2 + v_w \right]$$

The energy gained per cycle may be expressed as an altitude gain by noting that

$$\Delta h = \frac{E_a}{W}$$

It is now necessary to evaluate the energy dissipated to the atmosphere due to drag. For one complete cycle this is

$$(23) E_d = \int P_d dt = \frac{1}{\Omega} \int_0^{2\pi} P_d d\psi$$

where  $P_d$  is the power required to maintain level flight. If  $V$  is the flight speed and  $D$  the total drag at that speed.

$$P_d = VD$$

$$D = \frac{1}{2} \rho V^2 C_D S$$

$$C_D = C_{D_{\min}} + \frac{C_L^2}{\pi AR e}$$

$$C_L = \frac{L}{\frac{1}{2} \rho V^2 S}$$

$$D = \frac{1}{2} \rho V^2 S C_{D_{\min}} + \frac{L^2}{\frac{1}{2} \rho V^2 S \pi AR e}$$

In turning flight,  $L = nW$

$$n = \sqrt{\left(\frac{V\Omega}{g}\right)^2 + 1}$$

$$P_d = \frac{1}{2} \rho V^3 S C_{D_{\min}} + \frac{\left[\left(\frac{V\Omega}{g}\right)^2 + 1\right] W^2}{\frac{1}{2} \rho V S \pi AR e}$$

$$(24) P_d = \frac{1}{2} \rho S C_{D_{\min}} \left( \bar{v} + \frac{V\Omega}{2} \sin \psi \right)^3 + \frac{2W^2 \Omega^2 \left( \bar{v} + \frac{\Delta V}{2} \sin \psi \right)}{\rho S \pi AR e g^2} + \frac{2W^2}{\rho S \pi AR e \left( \bar{v} + \frac{\Delta V}{2} \sin \psi \right)}$$

Integration of equation (24) over one complete cycle yields

$$(25) E_d = \frac{1}{\Omega} \left[ \pi \rho S C_{D_{\min}} \left( \bar{v}^3 + \frac{3\bar{v}}{2} \left[ \frac{\Delta V}{2} \right]^2 \right) + \frac{4W^2}{\rho S AR e \sqrt{v_{\max} v_{\min}}} \right] + \Omega \left[ \frac{4W^2 \bar{v}}{\rho S AR e g^2} \right]$$

In level flight the minimum power required, or the minimum rate of sink for an unpowered aircraft, occurs at a speed at which

$$C_{D_{\min}} = \frac{1}{3} \frac{C_L^2}{\pi AR e}$$

If the minimum rate of sink,  $(R/S)_{\min}$ , and the speed at which that occurs,  $V_o$ , are known Equation (25) can be rewritten as

$$(26) \frac{E_d}{W} = \frac{\pi}{\Omega} \left[ \frac{(R/S)_{\min}^3}{2 V_o^3} \left( \bar{v}^3 + \frac{3\bar{v}}{2} \left[ \frac{\Delta V}{2} \right]^2 \right) + \frac{3(R/S)_{\min} V_o}{2 \sqrt{v_{\max} v_{\min}}} \right] + \Omega \pi \left[ \frac{3(R/S)_{\min} \bar{v} V_o}{2g^2} \right]$$

It will be recognized that  $\frac{E_d}{W}$  is the total altitude lost during one cycle. Equation (26) is of the form

$$\frac{E_d}{W} = \frac{A}{\Omega} + B\Omega$$

The turning rate for minimum altitude loss is

$$\Omega^2 = \frac{A}{B}$$

$$(27) \Omega^2 = \frac{g^2}{3V_o^4} \left[ \bar{v}^2 + \frac{3}{2} \left( \frac{\Delta V}{2} \right)^2 \right] + \frac{g^2}{\bar{v} \sqrt{v_{\max} v_{\min}}}$$

It is noteworthy that the optimum turning rate is independent of the minimum rate of sink and decreases as the speed for minimum rate of sink increases. There is another flight pattern which

also mimics the albatross. This is a combination of straight climbs into the wind and glides downwind, with a constant speed turn at the end of the climb or glide.

In the straight portions, the aircraft follows its natural Phugoid oscillation, climbing upwind and descending downwind.

Let the Phugoid oscillation frequency be  $f$ , and time zero occur when the aircraft is at its mean altitude heading downwind. Then

$$\delta = ft$$

$$h = \bar{h} - \frac{\Delta h}{2} \sin \delta$$

$$v = \bar{v} + \frac{\Delta v}{2} \sin \delta$$

$$\gamma = -\gamma_{\max} \cos \delta$$

The inertia force in a climb or glide due to wind shear is

$$F = \frac{W}{g} \frac{dv_w}{dh} \frac{dh}{dt}$$

and the power supplied to the aircraft relative to the air is

$$(28) \quad P_a = \left( \bar{v} + \frac{\Delta v}{2} \sin \delta \right) \left( \frac{W}{g} \frac{dv_w}{dh} \frac{dh}{dt} \right)$$

The rate of descent,  $\frac{dh}{dt}$ , may be evaluated similarly to the previous analysis.

$$\frac{dh}{dt} = - \left( \frac{dh}{dt} \right)_{\max} \cos \delta$$

$$dh = - \frac{1}{f} \left( \frac{dh}{dt} \right)_{\max} \cos \delta d\delta$$

$$\Delta h = - \frac{1}{f} \left( \frac{dh}{dt} \right)_{\max} \int_{\pi/2}^{\pi/2} \cos \delta d\delta$$

$$\Delta h = \frac{2}{f} \left( \frac{dh}{dt} \right)_{\max}$$

$$\left( \frac{dh}{dt} \right)_{\max} = \frac{f}{4g} (v_{\max}^2 - v_{\min}^2)$$

$$\frac{dh}{dt} = \frac{-f}{4g} (v_{\max}^2 - v_{\min}^2) \cos \delta$$

The equation (16) becomes

$$P_a = \frac{W}{g} \left[ \bar{v} + \frac{\Delta v}{2} \sin \delta \right]$$

$$\left[ \frac{-f}{4g} \frac{dv_w}{dh} (v_{\max}^2 - v_{\min}^2) \cos \delta \right]$$

The energy supplied by the wind during the glide is then

$$E_a = - \int P_a dt = - \frac{1}{f} \int_{-\pi/2}^{\pi/2} P_a d\delta$$

As noted earlier, for small  $\Delta h$  the wind velocity gradient can be taken as a constant. Then

$$E_a = \frac{2W}{g} \frac{dv_w}{dh} \left( \frac{\Delta v}{2} \right) \bar{v}^2$$

The energy supplied by the wind in a climb is the same. The total energy supplied in the straight portions of the cycle is then

$$E_a = \frac{4W}{g} \frac{dv_w}{dh} \left( \frac{\Delta v}{2} \right) \bar{v}^2$$

In a level turn the ground speed  $V_g = V + V_w \cos \psi$ . If the flight speed and windspeed are constant

$$\frac{dv_g}{dt} = -V_w \Omega \sin \psi$$

where  $\Omega$  is the turning rate.

The power supplied (or extracted) by the wind in the turn is then

$$P_a = -V \frac{W}{g} V_w \Omega \sin \psi$$

The energy gained in half a cycle is

$$E_a = -V V_w \int_{\pi}^0 \sin \psi d\psi$$

$$E_a = 2 V V_w \frac{W}{g}$$

In the second half of the cycle

$$E_a = -2 V V_w \frac{W}{g}$$

Thus, energy is gained in turning into the wind, and lost turning downwind, as previously observed.

The flight speed,  $V$ , is a maximum turning into the wind, and a minimum when turning downwind. The total energy gained or lost in the complete turn is then

$$E_a = 2 \frac{W}{g} \bar{v}_w \Delta v = 4 \frac{W}{g} \bar{v}_w \left( \frac{\Delta v}{2} \right)$$

Thus, the total energy for one complete cycle is

$$(29) \quad E_a = 4 \frac{W}{g} \left( \frac{\Delta v}{2} \right) \left[ \frac{1}{g} \frac{dv_w}{dh} \bar{v}^2 + v_w \right]$$

The energy supplied is thus seen to be more than that available in a circling orbit by a factor of  $\frac{4}{\pi}$ .

It is notable that the energy supplied is independent of either the Phugoid frequency or the turning rate in either case. It is dependent only on maximum

and minimum attainable flight speeds, the average wind velocity, and the wind velocity gradient.

The total energy dissipated to the atmosphere due to drag is of course not independent of either the Phugoid frequency of the turning rate.

For the straight portions of the flight

$$E_d = \int P_d dt = \frac{1}{f} \int_0^{2\pi} P_d d\delta$$

$$P_d = \frac{1}{2} \rho V^3 S C_{D_{\min}} + \frac{W^2}{\frac{1}{2} \rho V S \pi A R e}$$

Performing the indicated integrations yields

$$(30) \quad E_d = \frac{1}{f} \left[ \pi \rho S C_{D_{\min}} \left( \bar{v}^3 + \frac{3\bar{v}}{2} \left( \frac{\Delta v}{2} \right)^2 \right) + \frac{4W^2}{\rho S A R e \sqrt{v_{\max} v_{\min}}} \right]$$

In the turns

$$P_d = \frac{1}{2} \rho V^3 S C_{D_{\min}} + \frac{\left[ \left( \frac{V\Omega}{g} \right)^2 + 1 \right] W^2}{\frac{1}{2} \rho V S \pi A R e}$$

Integration over half a cycle gives the energy lost in each turn as

$$E_d = \frac{1}{\Omega} \left[ \frac{\pi \rho V^3 S C_{D_{\min}}}{2} + \frac{2W^2}{\rho V S \pi A R e} \right] + \frac{\Omega 2VW^2}{\rho S g^2 \pi A R e}$$

This expressions may be rewritten, as before, in terms of the minimum rate of sink. Then for the straight portion of the flight.

$$(30) \quad \frac{E_d}{Wd} = \frac{\pi}{f} \left[ \frac{(R/S)_{\min}}{2V_o^3} \right]$$

$$\left( \bar{v}^3 + \frac{3\bar{v}}{2} \left( \frac{\Delta v}{2} \right)^2 \right) + \frac{3(R/S)_{\min} V_o}{2 \sqrt{v_{\max} v_{\min}}}$$

And for the turns

$$(31) \quad \frac{E_d}{Wd} = \frac{\pi}{\Omega} \left[ \frac{(R/S)_{\min}}{4} \min \left( \frac{v}{\bar{v}} \right)^3 + \right]$$

$$\frac{3(R/S)_{\min}}{4} \min \left( \frac{V_o}{\bar{v}} \right) + \Omega \pi \left[ \frac{3(R/S)_{\min}}{4} \min \left( \frac{V_o}{g} \right) \right]$$

In this expression,  $V = V_{\min}$  for the turn at the high point of the orbit, and  $V = V_{\max}$  for the turn at the bottom. Equation (31) is of the form

$$\frac{E}{W}d = \frac{A}{\Omega} + \Omega B$$

The minimum loss of altitude occurs when

$$\Omega^2 = \frac{A}{B}$$

Then

$$(32) \left(\frac{E}{W}d\right)_{\min} = \frac{\pi (R/S)_{\min}}{2g} \sqrt{\frac{3V^4}{V_0^2} + 9V_0^2}$$

The total altitude lost is the sum of that given by Equation (30), and Equation (32) evaluated for each of the two turns.

### Experimental Results

The experimental investigation was conducted in a Beechcraft Bonanza Model F33-A aeroplane. This is a four place low wing single engine general aviation aircraft in the light utility category, equipped with a Continental IO-520-BA reciprocating engine developing a maximum of 285 horsepower at sea level, and a McCauley constant speed twoblade propeller.

The aeroplane was equipped with a drift sight located immediately behind the pilot's seat. This made it possible to measure drift angles on various headings and thus compute wind speed and direction at flight altitude.

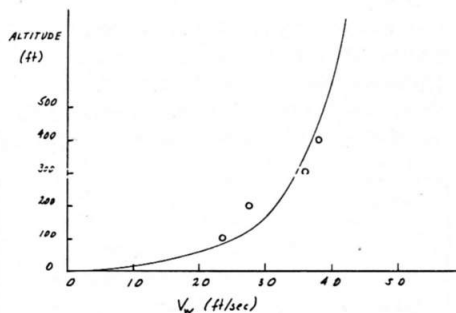


Fig. 5 Boundary Layer Shear

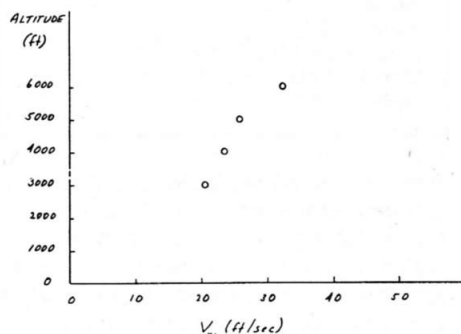


Fig. 6 Upper Atmosphere Shear

Figures 5 and 6 present the results of one set of such observations made on 24 March 1976 over the Chesapeake

Bay. Figure 5 is a plot of wind velocities below 1000 feet, the region which includes the atmospheric boundary layer, and Figure 6 shows the winds aloft. The velocity profile within the boundary layer agrees well with Davenport's power equation. The upper level wind velocity gradient was also found to be within the range of previously observed wind shears. (See Appendix I, Types of Wind Shear.)

The gain in altitude per cycle due to such wind shears by an aircraft emulating an albatross can be computed by reference to Equation (22) or (29); and the altitude lost due to drag from Equations (26) or (30) and (32).

The pertinent characteristics of the Beechcraft Bonanza aeroplane are summarized in Table 2. The power-off minimum rate of sink, and the speed at which this occurs, and stall speed, were determined by flight test.

Table 2

Stall speed, power off	74 MPH
Minimum R/S, power off	14.3 FT/S
Speed for minimum R/S	88 MPH
Design maneuvering speed	152 MPH

For the computations,  $V_{\max}$  was taken at 150 MPH, and  $V_{\min}$  at 80 MPH.

Table 3 presents the altitude which the aircraft could be expected to gain in one cycle from the wind conditions described above; and Table 4 the alti-

Table 3

Flight Altitude	$dV_w/dh$	Altitude Gain
3500	.00300	157 or 124
4500	.00225	170 or 133
5500	.00635	222 or 174
3000-6000	.00387	190 or 149
300	.04833	468 or 368

Table 4

Altitude Lost	Flight Pattern	
	Circling	Racetrack
793	1276	

tude which the Beechcraft Bonanza would lose per cycle due to drag. It is evident that for that for the Beechcraft Bonanza the altitude lost due to drag is far in excess of the gain due to wind shear. In fact, the wind shear would need to be about an order of magnitude greater for the gain to be the same as the loss.

The performance characteristics of the Beechcraft Bonanza can be altered, however, by the use of power. It can then be made to simulate high performance sailplanes. A convenient way to express the power supplied is as a percentage of the total thrust power

Table 5

Power %	$(R/S)_{\min}$ Ft/s	$(L/D)_{\max}$
0	14.3	11.57
15	9.8	15.28
20	8.0	18.89
25	6.0	23.66
30	4.5	31.27
35	3.0	48.37
40	1.5	97.73

available from the engine. Table 5 presents the equivalent performance parameters so obtained.

As a practical matter, it is more convenient simply to adjust the power as necessary to achieve the desired minimum

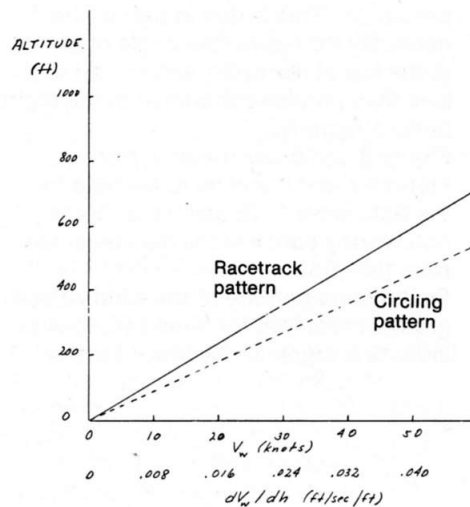


Fig. 7 Altitude Gained

sink rate. An advantage of this procedure is that it is then unnecessary to make any corrections to the test data for gross weight or a non-standard atmosphere when comparing experimental results with analytical predictions, as the minimum rate of descent and the altitude gained or lost are both determined for the same gross weight in the same atmosphere.

Figure 7 is a plot of the altitude which an aircraft may expect to gain as a function of wind shear. The latter is also expressed in terms of wind velocity at the 300 foot level, in order to give some feel for the wind velocities which might be required. The functional relationship between wind velocity and altitude was computed on the basis of Davenport's power equation.

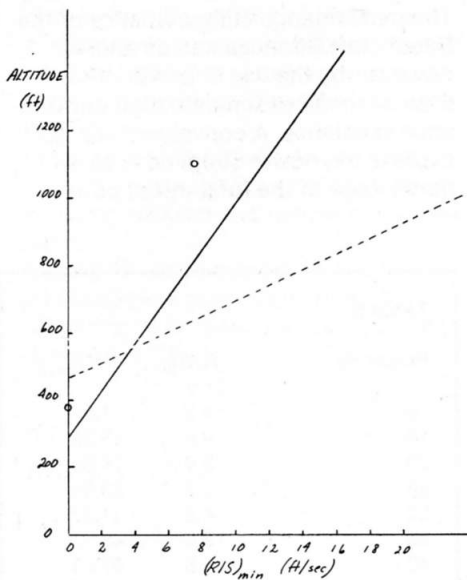


Fig. 8 Altitude Lost

Figure 8 is a plot of the altitude which the Beechcraft Bonanza may be expected to lose at various power settings. Two flight test data points are included for purposes of comparison. These were obtained under no-wind conditions, utilizing the racetrack pattern. It is evident that actual altitude lost is somewhat in excess of the analytic prediction. This is due in part to the necessity for easing the angle of bank at the top of the cycle, and in part to less than precise adherence to the flight pattern required.

Figure 9 combines the data from Figures 7 and 8 and includes data for the Schweizer 1-26 sailplane. Some noteworthy conclusions may be drawn from this plot. First, the magnitude of the wind velocity gradient required for a net zero loss of altitude is significantly lower for the

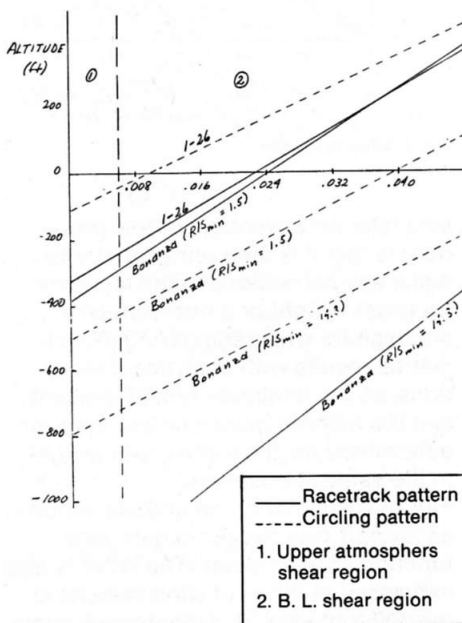


Fig. 9 Net Altitude Gained or Lost

circular pattern than it is for the racetrack pattern. Thus, pilot skill is an important factor.

Second, the wind shear required to achieve this balance is quite modest in the case of the Schweizer 1-26 sailplane, being on the order of .01 feet per second per foot. Reference to Table 3 shows that a greater wind shear than this was found to exist within the earth's boundary layer at 300 feet altitude. In fact, the wind velocity gradient was sufficiently steep so that the racetrack pattern would have served the 1-26 also.

It should be noted that the required angle of bank at the bottom of the cycle is quite steep, on the order of 75°. This should present no difficulty, however, since the load factor is well below the limit load factor. At the top of the cycle the required bank angle is 55°. This is well below that possible for the minimum speed selected, 40 MPH, and the level flight stalling speed.

Although Figure 9 shows that the Beechcraft Bonanza should be able to maintain continuous flight within a typical boundary layer wind shear when simulating a sailplane with a minimum rate of sink of one and a half feet per second, successful demonstration of this was not achieved. This was probably due to two factors: the mean altitude was generally too high, taking the flight pattern out of the steep part of the velocity gradient; and the flight precision required was not achieved.

### Flight Techniques

Although the racetrack flight pattern extracts more energy from the wind than does the circling pattern, as previously noted and as illustrated in Figure 7. Figure 8 shows that it is less efficient with respect to altitude lost due to drag. The circling pattern, however, is much more difficult to fly precisely. In the circling pattern it is necessary to ensure that flight speed is precisely at the required maximum when heading cross-wind at the minimum altitude, and at the required minimum when on the opposite heading at the top of the cycle. It must be the mean of these two values when heading directly downwind or upwind, at which time the angle of climb or descent must be a maximum. The turning rate must be kept constant at the computed optimum value, which means that the angle of bank must be varied continuously as flight speed changes.

The racetrack pattern is much less demanding of pilot skill. The technique which was developed is the following. Engine power is set for the desired rate of sink and the airplane is trimmed to fly hands-off at the mean flight speed, heading downwind. Speed is then reduced to the minimum without re-trimming and the controls are released. The nose will drop and speed will increase. When the speed is at trim speed the

angle of dive will be a maximum. Speed will continue to increase as the nose comes up, and it will be a maximum when the aircraft is in a level attitude. Thereafter the nose will continue to rise as the speed falls, again attaining trim speed when the climb angle is a maximum. As speed continues to fall, the nose will also, until level flight at minimum speed is once more established. The resulting Phugoid oscillation is timed, and maximum dive angle and speed are noted. If the maximum speed is below that desired elevator control is used in the next oscillation to increase the maximum dive angle. The dive angle needed to achieve the required maximum speed is noted.

On the next oscillation, when maximum speed is reached and the aircraft is heading downwind at the bottom of the cycle, it is put into a turn at the pre-computed bank angle, while the elevator control is used to maintain speed. After completing the turn into the wind wings are levelled and the elevator control is released. At the top of the cycle elevator control is again used to maintain minimum speed while the aircraft is turned downwind, when wings are again levelled and the elevator control is released. Elevator control is once more used to push the nose down a bit more if the maximum value required, as earlier determined, is not attained. Thus, flight speed is automatically varied in accordance with the normal Phugoid mode of the aircraft, with a little help from the pilot once each cycle to compensate for the normal damping of this mode.

This pattern can be flown quite precisely with a minimum of practice. Table 6 gives the flight parameters computed for the Beechcraft Bonanza for the circling and racetrack patterns.

	Pattern	
	Circling	Racetrack
Maximum speed	150 MPH	150 MPH
Minimum speed	80 MPH	80 MPH
Maximum load factor	2.12	2.14
Minimum load factor	1.41	1.49
Bank angle @ $V_{max}$	62°	62°
Bank angle @ $V_{min}$	45°	48°
Maximum dive angle	26°	17°

The maximum load factor presents no problem, since the design load factor for the Beechcraft at maximum gross weight is 4.4. The minimum load factor and the minimum speed are incompatible, however, because under these circumstances the stall angle of attack is exceeded. The problem can be solved by increasing the minimum speed or reducing the angle of bank. Equations (22) and (29) show that the energy

gained from the wind is directly proportional to the difference between maximum and minimum speed; increasing the minimum speed would reduce the energy gain significantly. A reduction in angle of bank, however, increases the energy loss due to drag far less. For example, a ten mile per hour increase in the minimum speed results in a 17% reduction in energy gained from the wind; whereas reducing the angle of bank from 48° to 30° produces a 5% increase in the altitude lost to drag. Accordingly, the top turn was generally made at 80 MPH, and the angle of bank was eased as necessary to avoid stall.

### Conclusions

1. There appears to be no theoretical bar to utilizing a vertical wind velocity gradient for obtaining continuous non-powered flight in existing sailplanes.
2. Wind velocity gradients which have been observed in the upper atmosphere are not sufficiently steep for this purpose. This may not be the case in the vicinity of a jet stream.
3. Wind velocity gradients within the boundary layer can provide the energy required for sustained non-powered flight in existing sailplanes. Surface winds of the order of 30 knots should be sufficient for this purpose.
4. Either a circular or a racetrack flight pattern may be utilized. The latter is more efficient in extracting energy from wind shear; the drag penalty, however, is greater. Overall, the circular pattern is more efficient but requires greater pilot skill.
5. Precision in following the prescribed flight pattern is of utmost importance. The circular pattern is most demanding in this respect. In the racetrack pattern, in the turns angle of bank must be held constant; in the turn at the top airspeed must not be allowed to increase, nor must it be allowed to decrease in the bottom turn. There is a strong urge to do both; in the one case to avoid stall, and in the other due to a rapid rate of descent close to the ground. Since the energy lost to drag is a function of the pattern period, the time in a turn must not be increased by reducing the bank angle. The energy gained from wind shear depends on the magnitude of difference between maximum and minimum flight speed; it is therefore important not to decrease the former or increase the latter.

### Appendix I Types of Wind Shear

#### Introduction

Numerous articles have been written dealing with the meteorological phenomenon known as wind shear. Wind shear is a velocity gradient with increas-

ing altitude; a wind profile which must exist in order to account for the difference between relatively large upper atmosphere winds and the air at the earth's surface which is essentially at rest.

Such a wind differential has become an important design consideration of modern skyscrapers. Structural allowances must be made for the increased wind loading experienced by tall buildings.<sup>1</sup> Recently studies concerning the effects of velocity gradients upon landing aircraft have been undertaken. The National Aeronautics and Space Administration sponsored an investigation into such effects<sup>2</sup>. Analytic studies utilizing a digital computer simulation show that wind shear produces a significant deviation in the touchdown point of a landing aircraft as compared to the same aircraft landing under exactly the same conditions except for the absence of shear<sup>3</sup>. Additionally, the National Transportation Safety Board acknowledged wind shear as a primary contributor to the crash of an Iberia airliner on December 17, 1973<sup>4</sup>. Therefore the existence of velocity gradients has emerged in recent years as an important engineering consideration.

#### Types Of Wind Shear

Evidence suggests that there exist two characteristic types of wind shear. The first is found near the earth's surface and closely resembles the shape of a typical viscous flow boundary layer. Beyond the well defined boundary layer, however, is a more subtle, gradually increasing velocity gradient. This gradient has been referred to as upper level shear.

#### Boundary Layer Shear

A great deal of research has been done on the subject of the earth's boundary layer shear. This is probably due to the previously mentioned importance of boundary layer shear in recent engineering considerations and its relative ease of measurement due to its close proximity to the ground.

Boundary layer shear is a relatively common occurrence because of its dependence upon surface friction effects rather than prevailing weather conditions. The single major exception to this generalization is pointed out by Mr. Davenport in his initial study of boundary layer shear. He found that in severe thunderstorms or squalls the boundary layer breaks down. Under such violent frontal conditions the atmosphere directly above the earth is highly turbulent and unstable, the result being that a distinct, gradient style increase in velocity with altitude is greatly reduced<sup>5</sup>. The boundary layer may usually be expected to be somewhat turbulent.

Obstructions such as buildings, hills and trees give rise to gyrating vortices and vertical thermal currents further add to the instability of the boundary layer.

Various formulas have been suggested to describe the wind profile in the boundary layer but the most popular is the power equation;

$$V(z) = kz^{1/a}$$

where  $V(z)$  is the wind velocity at altitude  $z$ ,  $k$  is a strength coefficient which must be determined experimentally, and  $a$  is dependant upon the terrain (i.e. surface roughness). Based upon extensive worldwide research Mr. Davenport<sup>6</sup> offers the following guidelines for assigning a value to  $a$  (see Fig. 1):

1. open country, flat lands, grassland, large bodies of water and tundra;  $a=7$ .
2. wooded countryside, rough coastal belt, outskirts of a city;  $a=3.5$ .
3. center of a large city;  $a=2.5$ .

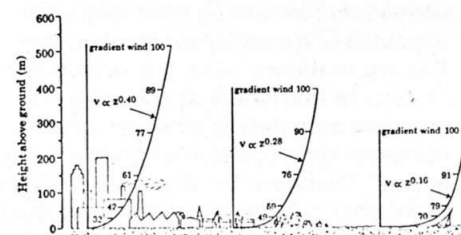
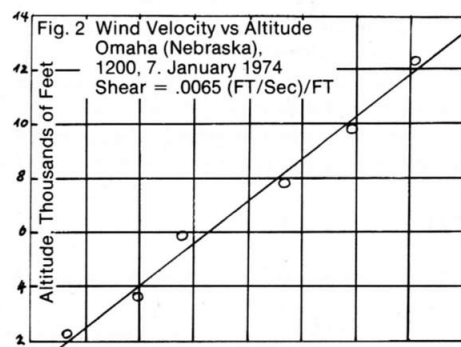


Fig. 1 Wind profiles described by Davenport's power equation parameters over various terrain.

#### Upper Level Shear

Analytic research concerning upper level shear has been much less extensive than for boundary layer shear. High altitude shear requires much more sophisticated measuring systems and is of less direct engineering importance due to its relative weakness and its distance from the earth's surface. Actual meteorological data confirms the existence of upper level wind shear. Figure 2 displays a velocity gradient which occurred over Omaha in January, 1974. The strength of the gradient was 0.0065 ft/sec · ft<sup>7</sup>. Two important characteristics may be noted about the non-boundary layer shear described in Figure 2. First, as mentioned previously,



the gradient is quite weak, increasing only 0.65 ft/sec in every 100 feet. This fact alone suggests that detection and accurate measurement of upper level shear would demand painstaking care. Secondly, the velocity gradient above the boundary layer may reasonably be presented by a straight line function.

In order to achieve maximum efficiency from flying time for this report it was necessary to determine exactly what type of weather conditions would prove most advantageous for detecting and measuring the velocity gradient. In particular, a forecast outline for wind shear was needed for the Virginia and Maryland area where data flights were to be made.

Mr. W. Bonner discussed the characteristics of low level wind maxima in an article written for *Monthly Weather Review*.

Though the thrust of the article was aimed at commenting on characteristics of the boundary layer particular to the midwest, the author made valuable comments concerning what might be expected of a velocity gradient on the Eastern seaboard. Also, it is reasonable to assume that where and when a pronounced boundary layer shear exists, a corresponding upper level gradient may appear. Therefore Mr. Bonner's analysis of weather conditions creating low level shear may also be applied to predicting upper level shear. His study was based on data taken from forty-seven weather stations (including several in the Maryland, Virginia and Delaware areas) during a two year time span at a rate of two observations per day.

In general, the velocity gradients were more frequently observed in the morning hours. Though in the midwest there was a definite increase in low level shear during the summer months, no such precise generalization could be made concerning the East. Actually, the velocity gradient seemed to be more abundant in the Annapolis area between the months of October and March. In addition, such a velocity gradient was usually from the north or northwest<sup>8</sup>.

An independent U.S. Army Missile Command report supports Mr. Bonner's observations. It shows an increase in the strength of the shear in the vicinity of Annapolis's longitude during the fall and winter months<sup>9</sup>. Figure 3 is a graphical display of some of the results of this report.

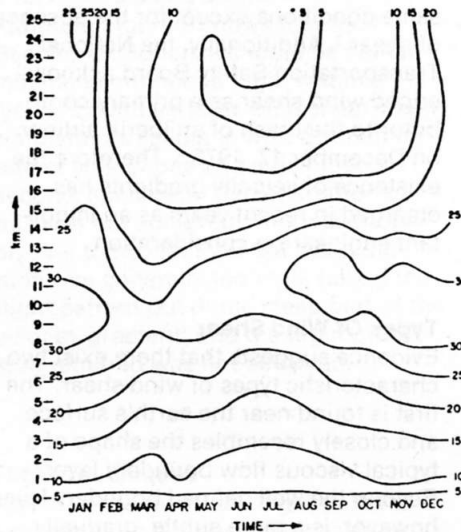


Fig. 3 Time section of wind shear (m/sec/km) near longitude 80°W. Annapolis longitude is approximately 76°30'W.

#### Footnotes

<sup>1</sup> Hans Thomann, "Wind Effects On Buildings and Structures", *American Scientist*, 63 (1975), 278-287.

<sup>2</sup> James Luers and Jerry Reeves, "Effect of Shear on Aircraft Landing", CR-2287, July 1973, NASA.

<sup>3</sup> James Luers and Jerry Reeves, "Wind Shear Effects on the Landing of Aircraft", *Journal of Aircraft*, 12 (July 1975), 565-566.

<sup>4</sup> "NTSB Assays Iberia Accident at Logan", *Aviation Week and Space Technology*, 102 (7 April 1975), 54.

<sup>5</sup> A.G. Davenport, "Rationale For Determining Design Wind Velocities", *Journal of the Structural Division, Proceedings of the American Society of Civil Engineers*, 86 (May 1960), 43.

<sup>6</sup> Davenport, p. 48.

<sup>7</sup> U.S. Department of Commerce, National Oceanic and Atmospheric Administration, Summary of Constant Pressure Data (WBAN 33), January 7, 1974.

<sup>8</sup> W. Bonner, "Climatology of the Low Level Jet", *Monthly Weather Review*, 96 (1968), 833-850.

<sup>9</sup> Dorothy Anne Stewart, "A Note On Wind Shear Near 80 W", *Journal of Applied Meteorology*, 6 (August 1967), 724.

#### List of References

- Bonner, W. "Climatology of the Low Level Jet", *Monthly Weather Review*, 96 (1968), 833-850.
- Davenport, A.G., "Rationale For Determining Design Wind Velocities", *Journal of the Structural Division, Proceedings of the American Society of Civil Engineers*, 86 (May 1960), 43.
- Luers, James and Jerry Reeves, "Effect of Shear on Aircraft Landing", CR-2287, July 1973, NASA.
- Luers, James and Jerry Reeves, "Wind Shear Effects on the Landing of Aircraft", *Journal of Aircraft*, 12 (July 1975), 565-566.
- "NTSB Assays Iberia Accident at Logan", *Aviation Week and Space Technology*, 102 (7 April 1975), 54.
- Stewart, Dorothy Anne, "A Note On Wind Shear Near 80 W", *Journal of Applied Meteorology*, 6 (August 1967), 724.
- Thomann, Hans, "Wind Effects On Buildings and Structures", *American Scientist*, 63 (1975), 278-287.
- US Department of Commerce, National Oceanic and Atmospheric Administration, Summary of Constant Pressure Data (WBAN 33), January 7, 1974.